COMPDYN 2015
5th ECCOMAS Thematic Conference on
Computational Methods in Structural Dynamics and Earthquake Engineering
M. Papadrakakis, V. Papadopoulos, V. Plevris (eds.)
Crete Island, Greece, 25–27 May 2015

OPTIMAL DESIGN OF STRUCTURAL INTERFACES BY A POWER FLOW MODE APPROACH

Thomas Weisser[1], **Noureddine Bouhaddi**[2]

[1]MIPS Laboratory, Université de Haute-Alsace
12 rue des Frères Lumière, 68093 Mulhouse, FRANCE
thomas.weisser@uha.fr

[2] Applied Mechanics Department, FEMTO-ST Institute
24 chemin de l'Épitaphe, 25000 Besançon, FRANCE
noureddine.bouhaddi@univ-fcomte.fr

Keywords: Structural Dynamics, Complex Structures, Power Flow, Optimization, Robustness.

Abstract. *Complex mechanical structures usually encountered in the automotive or aerospace industries are composed of an assembly of several components, often exhibiting different mechanical properties and joined at their interfaces by different junction types. The various dynamic behaviors of these substructures and the applied external loadings may generate important forces on the main structure, resulting in high acceleration responses of the on-board equipment, potentially affecting their performance, reliability and security. It is therefore necessary to protect these components from these harsh interface loadings by isolating them from the rest of the structure.*

A variant of power flow mode methods, dedicated to low frequency vibrations, is presented which enables to dynamically characterize these structural interfaces. It is based on the imaginary part of the dynamic flexibility matrix, allowing to determine eigenvalues and eigenforces which represent qualitative and quantitative information on the power flowing inside the structure, respectively. This method is applied to study the power transmitted at the interface, making it possible to identify the direction associated to some dominant power flow patterns and to quantify their contributions. An optimal design procedure of such interfaces, with regard to their mechanical parameters (i.e. stiffness), is further proposed. Both mono-objective and robust multi-objective procedures are implemented and compared to optimize the derived power flow variables. The whole procedure is applied to a simplified coupled structure illustrating structural vibration phenomena on space-launchers.

1 INTRODUCTION

From the early stages of the design process of industrial mechanical structures, such as encountered in the aerospace or automotive sectors, it is necessary to ensure the correct dimensioning of their various components as well as their assembly, to satisfy the expected performance criteria. Given the diversity of the associated structural dynamic behaviors, vibration isolation issues are likely to occur which may finally impact the performance, reliability and security of the whole structure.

The vibration transmission between the boosters and the rocket core of the European space launcher *Ariane 5* perfectly illustrates this stake. During the atmospheric flight, combustion of the solid propellant excites acoustic modes of the boosters resulting in harmonic oscillations of their structures. One of these modes induces an important dynamic response at the junction with the rocket core, which could have an impact on the dynamic environment [2]. For such reasons, industrials need to have access to design procedures to determine optimal power flow paths and thus to ensure vibration isolation.

Such procedures consist in defining one or several cost functions, which are often complex with regard to the design parameters (multi-modal, non-convex,...) and usually contradictory. While eventually convincing, the derived solutions may be particularly sensitive to even small perturbations: it is thus necessary to consider the robustness of these solutions. This can be handled by simultaneously minimizing both average μ_f and standard deviation σ_f of a cost function f, using a vulnerability function f_v defined by

$$f_v = \frac{\sigma_f}{\mu_f} = \frac{1}{f_r} \tag{1}$$

and corresponding to the inverse of the robustness function f_r [1]. The optimization problem thus becomes a multi-objective one, consisting in minimizing one or several cost functions and their associated vulnerability functions, to derive a set of Pareto-optimal (non-dominated) solutions. As genetic algorithms seem particularly well adapted to such problems, a Non Sorted Genetic Algorithm (NSGA) initially developed by Srinivas [9] will be further used in this study.

As previously exposed, vibration isolation problems amount to minimizing the vibration transmitted from a source substructure to a receiver one. The computations exposed in this study are based on a power flow mode approach, as initially proposed by Su *et al.* [10]. Deriving from the seminal works of Goyder and White [4] and Miller *et al.* [7] concerning power flow analysis, the authors have complemented these approaches by the multipole method developed by Pinnington [8] and frequency synthesis techniques to propose a mobility-based power flow mode method. This method mainly consists in transforming a set of source forces or velocities into a new set of power flows: these are associated to modal forces or velocities weighted by orthogonal functions derived from the eigenproblem of a mobility matrix [10].

The targeted applications of this study mainly refer to low frequency structural vibrations of complex structures. Hence, the power flow mode approach has been adapted to combine the advantages of both finite element analysis, *i.e.* fine spatial description, complex geometry handling, vector quantities, and power flow analysis, *i.e.* quadratic variables and scalar characteristic quantities: based on a displacement formulation, this aims to derive power flow modes to qualitatively and quantitatively characterize interface forces in order to estimate their ability to transmit power flow between components[12]. This method is briefly presented in the next section and will be further integrated into the optimization procedure.

2 POWER FLOW MODE METHOD

2.1 Theoretical formulation

The proposed power flow mode method aims to characterize the interface forces between two components of a coupled structure: a source substructure, denoted (*S*), submitted to an external loading $\mathbf{f}^{(S)}$ and a passive receiver substructure, denoted (*R*). The dynamic equilibrium equation of the whole structure is given by:

$$\begin{bmatrix} \mathbf{Z}_{ii}^{(S)} & \mathbf{Z}_{ij}^{(S)} & \mathbf{0} \\ \mathbf{Z}_{ji}^{(S)} & \mathbf{Z}_{jj}^{(S)} + \mathbf{Z}_{jj}^{(R)} & \mathbf{Z}_{ji}^{(R)} \\ \mathbf{0} & \mathbf{Z}_{ji}^{(R)} & \mathbf{Z}_{ii}^{(R)} \end{bmatrix} \begin{pmatrix} \mathbf{x}_i^{(S)} \\ \mathbf{x}_j \\ \mathbf{x}_i^{(R)} \end{pmatrix} = \begin{pmatrix} \mathbf{f}_i^{(S)} \\ \mathbf{0} \\ \mathbf{0} \end{pmatrix} \tag{2}$$

where subscripts *i* and *j* respectively denote internal and junction degrees of freedom (*DOFs*), $\mathbf{Z}^{(.)}$ is the frequency dependent dynamic stiffness matrix of a substructure and $\mathbf{x}^{(.)}$ its dynamic response.

To determine the power flow modes associated to the junction *DOFs*, the power transmitted between both substructures must be expressed with regard to the interface variables. As classically detailed in the work of Bobrovnitskii [3] this average power flow, in harmonic state at a given frequency ω_0, can be derived from the real part of the complex power:

$$P_j^{tr}(\omega_0) = \frac{1}{2}\Re\mathrm{e}\left\{\mathbf{f}_j^H \mathbf{v}_j\right\} = \frac{j\omega}{4}\left(\mathbf{f}_j^H \mathbf{x}_j + \mathbf{x}_j^H \mathbf{f}_j\right) \tag{3}$$

By decoupling equation (2) and considering the classic compatibility equations, this average power flow can be expressed as a quadratic form,

$$P_j^{tr}(\omega_0) = -\frac{\omega_0}{2}\mathbf{f}_j^H \Im\mathrm{m}\left\{\mathbf{\Gamma}_{jj}^{(R)}(\omega_0)\right\}\mathbf{f}_j \tag{4}$$

where $\mathbf{\Gamma}_{jj}^{(R)} \in \mathbb{C}^{(N_j,N_j)}$ corresponds to the dynamic flexibility matrix of the receiver substructure, restricted to its junction *DOFs*:

$$\mathbf{\Gamma}_{jj}^{(R)} = \left[\mathbf{Z}_{jj}^{(R)} - \mathbf{Z}_{ji}^{(R)}\left[\mathbf{Z}_{ii}^{(R)}\right]^{-1}\mathbf{Z}_{ij}^{(R)}\right]^{-1} \tag{5}$$

Hence, minimizing equation (4) at each considered frequency with regard to the interface forces amounts to solving the following equivalent eigenproblem:

$$\left[\Im\mathrm{m}\left\{\mathbf{\Gamma}_{jj}^{(R)}(\omega_0)\right\} - s_\nu \mathbf{I}_{N_j}\right] g_\nu = 0\,, \quad \nu = 1, \ldots, N_j \tag{6}$$

where N_j denotes the number of junction *DOFs*[1]. This equation only depends on the physical parameters of the receiver and the frequency: the derived power flow modes, comprising the eigenvalues s_ν and the associated eigenforces g_ν, are independent of the interface forces applied by the source substructure to the receiver one, thus allowing to characterize the power potentially transmitted at the interface.

[1]To ease further readability, the following notation is adopted: $\mathbf{\Gamma}^{\Im} = \Im\mathrm{m}\left\{\mathbf{\Gamma}_{jj}^{(R)}\right\}$.

Therefore, at each considered frequency, the basis of the eigenforces spans the whole power flow pattern space associated to the interface: these eigenvectors represent the prevailing directions or paths through which the power proportional to the associated eigenvalues will flow. It is thus possible to decompose the actual interface forces $\mathbf{f}_j \in \mathbb{C}^{(N_j,1)}$ as a linear combination:

$$\mathbf{f}_j = \sum_{\nu=1}^{N_j} \alpha_\nu \mathbf{g}_\nu \tag{7}$$

where α_ν are complex projection coefficients representing the contribution of each eigenforces $\mathbf{g}_\nu$ in $\mathbf{f}_j$. This allows to express the power transmitted at the interface (equation (3)) as the sum of the power independently transmitted by each of the N_j power flow modes,

$$P_j^{tr}(\omega_0) = -\frac{\omega_0}{2}\mathbf{f}_j^H \, \mathbf{\Gamma}^{\Im}(\omega_0) \, \mathbf{f}_j = -\frac{\omega_0}{2}\sum_{\nu=1}^{N_j} |\alpha_\nu|^2 s_\nu > 0 \tag{8}$$

where $P_\nu(\omega_0) = -\frac{\omega_0}{2}|\alpha_\nu|^2 s_\nu$ is referred to as the modal power flow.

2.2 Application

To illustrate the previously described industrial context, a finite element model representing a simplified space launcher structure, depicted figure 1 (a), has been designed. The junction between the different cylinders representing the main core and each booster are modeled by three translational springs along the global coordinate system axis. Their location respects the topology of the actually adopted technical solutions, corresponding to three junctions at each of the lower interface and one junction at each upper interface. To simplify the model and to limit the number of design parameters (12 instead of 24), the junctions are supposed symmetrical about the main core axis. However, considering the difficulty to estimate values of these stiffness parameters and to avoid saturation effects resulting in insensitive dynamic responses, a sensitizing input procedure [11] has been used to determine there initial values, given table 1.

Dir.	Junction 1	Junction 2	Junction 3	Junction 4
T_x	2.9315e9	1.2328e9	2.1963e9	1e12
T_y	5.8617e9	1.404e11	1.394e10	1e12
T_z	1.7433e9	2.1963e9	2.4652e9	1e12

Table 1: Initial values of the interface stiffness parameters (N/m)

Moreover, for practical considerations the structure, including junctions, is globally submitted to a proportional damping hypothesis. Finally, to observe a dynamic behavior similar to the actual one, a harmonic in-phase load is applied to the boosters as a unitary axial force distributed between the lower and upper junctions, coupled to a small out-of-phase transverse perturbation.

Figure 1 (a) shows the evolution of the 24 power flow eigenvalues associated to the interface *DOFs*. The presence of amplitude resonances confirms the important amount of power

transmitted over this frequency band, especially between 45 Hz and 55 Hz where two normal vibration modes are located. These correspond to flexural modes of the boosters as depicted figure 1 (b) by the colormap representing the strain energy distribution. Moreover, only a third of these eigenvalues exhibits a frequency behavior between 0-100 Hz: these may constitute a dominant subspace. This figure also shows the eigenvectors associated to the 3^{rd} power flow mode at 52 Hz, depicting the strain energy of the interfaces, and the 7^{th} one which is orthogonal by definition and whose power flow pattern is less active (*cf.* associated eigenvalue).

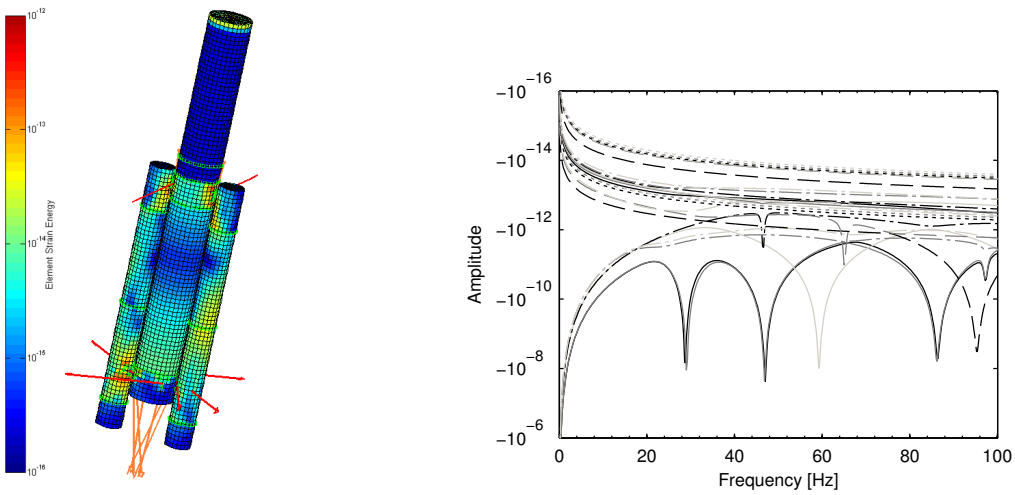

(a) Eigenforces g_3 and g_7 at 52 Hz (b) Power flow eigenvalues of the receiving substructure $-$ s_1, $-$ s_2, $-$ s_3, $--$ s_4, *etc.*

Figure 1: Initial power flow modes at the interface of the test-structure

Finally, figure 2 shows the frequency evolution of each modal power flow, whose summed amplitudes have been unitary normalized. It can be observed that the subspace spanned by power flow modes 3, 6 and 8 comprises more than 60 $\%$ of the power transmitted bewteen the boosters and the main core of the test-structure. As a result, these quantities associated to the dominant power flow paths seem particularily relevant in the context of a design optimization procedure.

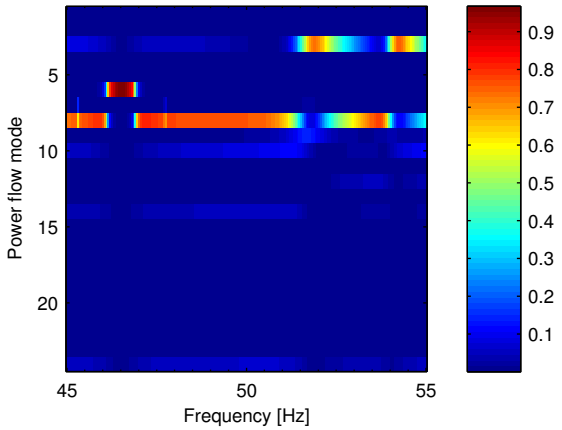

Figure 2: Initial modal power flows P_ν

3 TRANSMITTED POWER FLOW OPTIMIZATION

3.1 Determination of the cost function

According to the previous comments, the cost function f_c to be minimized during the optimization process is defined as:

$$\min_{\mathbf{X}} f_c = \min_{\mathbf{X}} \left(\max_{\omega} \frac{\sum_{\nu=1}^{6} P_\nu(\omega)}{P_j^{tr}(\omega)} \right) = \min_{\mathbf{X}} \left(\max_{\omega} \frac{\sum_{\nu=1}^{6} |\alpha_\nu|^2 s_\nu}{\sum_{\nu=1}^{24} |\alpha_\nu|^2 s_\nu} \right) \tag{9}$$

where $\mathbf{X} \in \mathbb{R}^{(12,1)}$ denotes the vector of the design parameters (*i.e.* junction stiffnesses). This function represents the maximum contribution of the power flow paths spanning the subspace comprising the six first power flow modes. Minimizing this function amounts to projecting the real interface forces along the directions associated to the less important power flow paths. However it must be noticed that the 8^{th} mode has not been retained to avoid over-constraining the optimization problem: although part of the prevailing paths, it potentially concentrates the smaller power flow as $|s_8| < \ldots \ll |s_1|$ while remaining sensitive to the design parameters. It thus constitutes an effective alternative for the power flow diverted from the other dominant paths, which could lower the power transmission.

3.2 Mono-objective approach

The first proposed approach consists in a deterministic optimization procedure whose flowchart is detailed figure 3. A preliminary Monte-Carlo analysis based on 300 samples has been performed to determine some relevant starting points. Based on the obtained initial parameter sets, the gradient-based nonlinear programming algorithm *fmincon* included in the Matlab Optimization Toolbox [5] is used to minimize the cost function: at each iteration the most sensitive direction is sought to converge toward a local minimum.

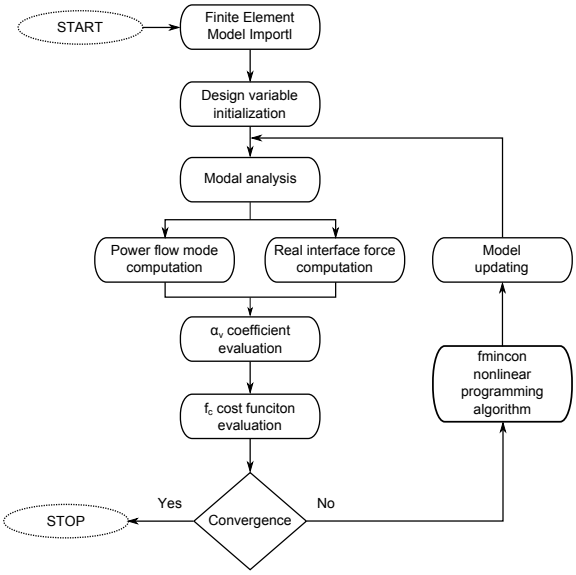

Figure 3: Flowchart of the mono-objective optimization procedure

As an example, figures 4 (a) and (b) respectively represent the evolution of the design variables and the cost function for a starting point with $f_c = 75.75\%$. The different steps of the local sensitivity analysis can be observed before each drop of the cost function, which convergences

after 215 iterations. The results derived from each of the three retained starting points are given table 2 in relative terms. It can be noticed that the final values reached by the cost function are independent of the initial ones, as these do not guarantee the accuracy of the closest local minimum: it may be possible to reach a better solution starting from a worse initial point. The resolution will however be more time consuming and computationally cost effective.

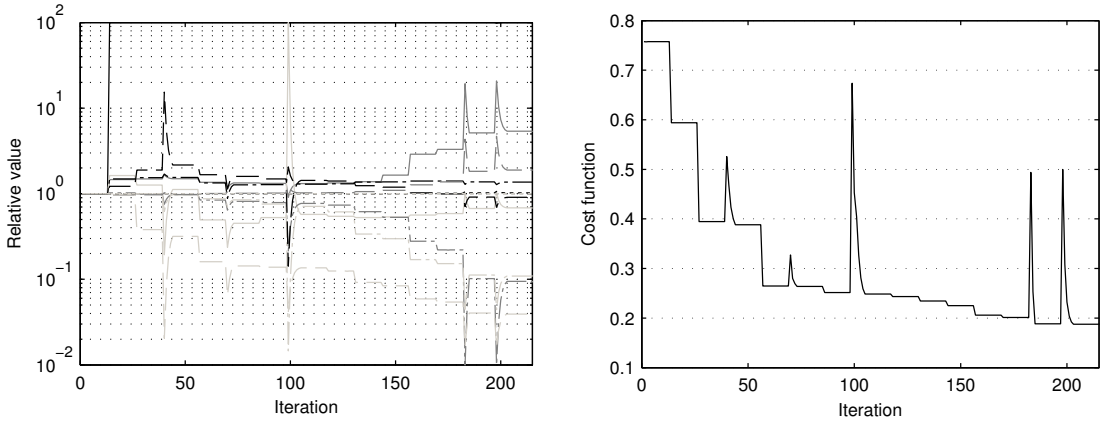

(a) Evolution of the design parameters (b) Evolution of the cost function

Figure 4: Evolution of the mono-objective optimization starting from point 195

Point	f_c (%)	**Direction**	**Junction 1**	**2**	**3**	**4**
238	45.15 → 23.64	T_x	8.19	95.79	5.77	0.01
		T_y	1.26	1.38	79.2	2.78
		T_z	8.17	0.47	10.07	0.02
262	70.63 → 27.91	T_x	4.82	61.5	11.68	3.5
		T_y	0.03	0.16	0.01	7.86
		T_z	2.28	14.77	20.6	0.52
195	75.75 → 18.74	T_x	100	54.2	0.8	13.64
		T_y	55.36	0	0.05	6.62
		T_z	2.02	5.74	0.01	25.61

Table 2: Relative values of the optimal interface stiffness parameters (mono-objective optimization)

At first sight, these results do not look very similar to one another. Moreover, some design variables have reached the bounds of their dispersion interval: such design points may be standing on a slope leading to a better solution. It can be verified, figure 5 (a), that the derived optimal values of the design parameters actually lower the maximum amplitude of the power flow transmitted at the interface, between $45 - 55\ Hz$. However the associated frequency evolutions tend to be quite different in each case. The same applies to the acceleration response levels displayed figure 5 (b). While a reduction of the amplitude is locally achieved, considerable modifications of the dynamic response can be observed at other frequencies: some power flow resonances

tend to vanish, others are amplified and similarly some vibration modes are highly shifted in frequency. This could possibly lead to new unwanted adverse effects perturbing the structure.

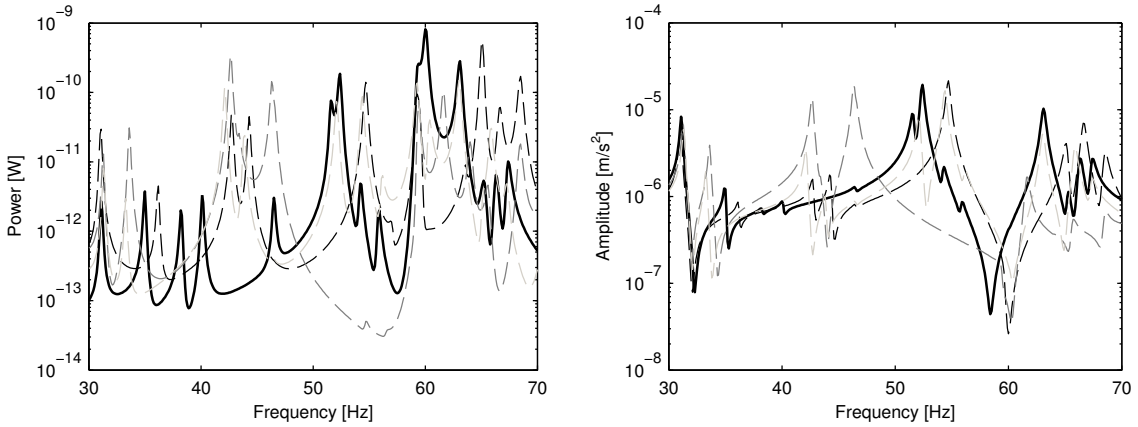

(a) Power flow transmitted at the interface

(b) Acceleration response level of the main core (vertical direction)

Figure 5: Results of the mono-objective optimization procedure:
— initial ; optima _ 1, −− 2, −− 3

Hence, while all these solutions verify the optimization problem and minimize the cost function f_c, it is necessary for the designer to choose the best one considering the global frequency behavior of the coupled structure. Therefore, it may be appropriate to add some design constraints, for example concerning the maximum frequency shift of sensitive vibration modes or response levels not be exceeded, in order to avoid particular types of solutions.

3.3 Robust multi-objective approach

In this section, a robust multi-objective approach is applied to optimize both the cost function f_c and its vulnerability function f_v, defined equation 1. This numerical procedure is detailed in the flowchart figure 6 (a). As previously emphasized, it is based on a genetic algorithm whose parameters have been set as follows [9]: 50 individual solutions per generation; a crossover probability $p_c = 0.8$; a mutation probability $p_m = 0.1$; a parameter of niche function $\sigma = 0.2$.

The major drawback of this approach stems from the evaluation of the vulnerability function. Indeed, it is necessary to locally determine, for each individual, the average and standard deviation of the cost function. These computations are performed considering 50 Monte-Carlo samples, with a uniform distribution and a dispersion of 10 $\%$. However, it implies to successively derive the associated real interface forces: computational costs are thus reduced by using a modal superposition approach, coupled to an approximated realanalysis technique based on an enrichment of the initial basis with static residuals [6].

The results from this robust multi-objective optimization are illustrated figure 6 (b), for two different runs: the first one converged after only 7 generations (16 hours) and the second one after 14 generations (24 hours)[2]. Both complete sets of solutions are depicted. At first, it can be noticed that a large amount of inefficient but robust individuals has been derived, while only a few ones verify $f_c < 40\%$. Moreover, the obtained Pareto fronts turn out to be relatively sparse (with respectively 13 and 14 individuals) but quite homogeneous.

[2]All numerical simulations have been performed using a 3 GHz dual-core processor with 1.96 $Go\ RAM$.

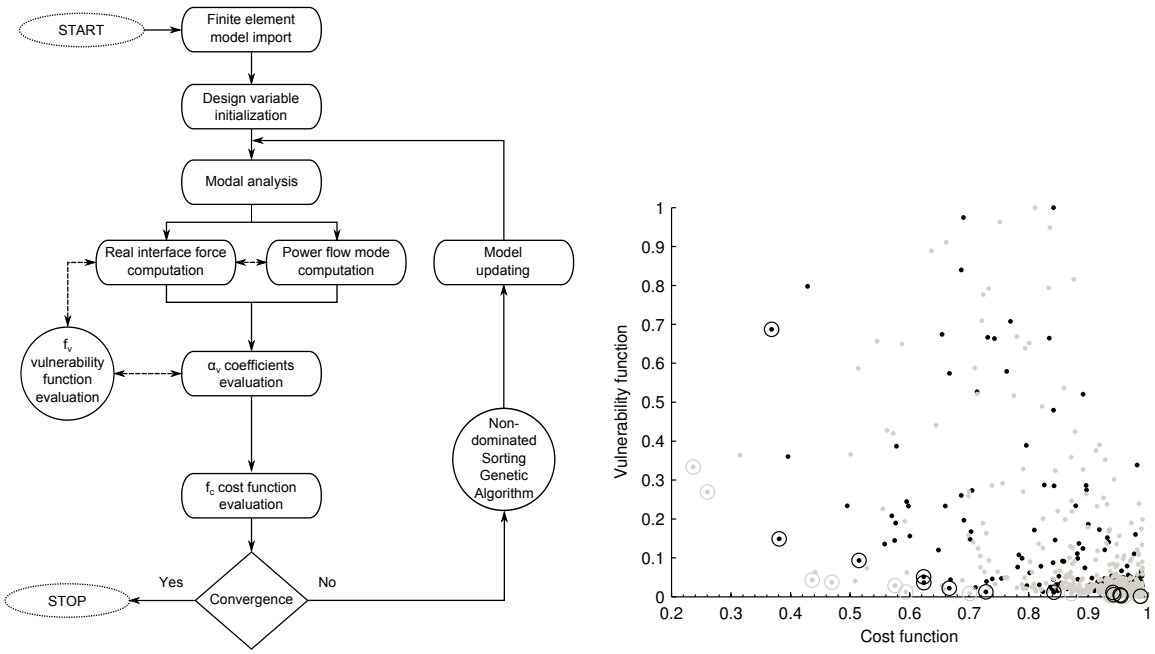

(a) Flowchart of the procedure

(b) Solutions and Pareto-fronts
$\cdot \odot$ 1^{st} run, $\cdot \odot$ 2^{nd} run

Figure 6: Robust multi-objective optimization procedure

The values of the design parameters associated to the four points belonging to the Pareto fronts and constituting the best trade-off between performance and robustness are given table 3, in relative terms. Once again these solutions seem to differ from one another and some design variables have reached the bounds of their dispersion interval. However, figure 7 (a) clearly shows that each of them leads to a reduction of the transmitted power on the considered frequency band, as well as a lowering of the acceleration response level at the top of the main core, figure 7 (b). It can be noticed that these optimal designs seem to modify the global dynamic behavior of the coupled structure in the same way, corresponding to a stiffening of the vibration modes initially located around 55 Hz, with a significant reduction of the power flow resonance at 60 Hz (excepted for solution 3).

This procedure thus managed to find efficient solutions to the optimization problem, which are also different from the previous ones derived by the mono-objective approach. These solutions tend to be more conservative with regard to the initial dynamic behavior of the structure.

4 CONCLUSION

A robust design approach has been presented to optimize structural interfaces between a source and a receiver substructure of a complex mechanical structure. The obtained results have shown an interest in using power flow modes to derive solutions that minimize the transmitted power flow. Indeed, this method allows to identify interface force distributions constituting prevailing power flow paths which can be avoided by appropriately tuning the interface stiffness parameters. A mono-objective procedure based on a deterministic algorithm has been compared to a multi-objective one, taking into account the vulnerability of the solutions, using Non-Sorted Genetic Algorithm. Both have been applied to a representative complex structure and have achieved interesting designs which actually reduce the vibration response level of the receiver substructure.

Point	$[f_c - f_v]$ (%)	**Dir.**	**Junction 1**	**Junction 2**	**Junction 3**	**Junction 4**
428	23.63 - 33.32	T_x	4.4	52.54	1.82	6.8
		T_y	5.7	3.43	1.02	100
		T_z	48.07	3.15	13.97	0.13
505	26.04 - 26.93	T_x	22.63	100	5.94	63.85
		T_y	0.42	4.96	37.49	2.16
		T_z	2.27	0.53	0.15	74.77
157	38.09 - 14.87	T_x	70.48	87.12	0.01	1.01
		T_y	41.8	0.01	18.56	14.91
		T_z	39.81	7.04	2.85	0.91
176	43.63 - 4.28	T_x	17.42	74.21	2.07	0.35
		T_y	16.96	1.83	0.01	2.33
		T_z	0.11	53.86	1.42	0.24

Table 3: Relative values of the optimal interface stiffness parameters (multi-objective optimization)

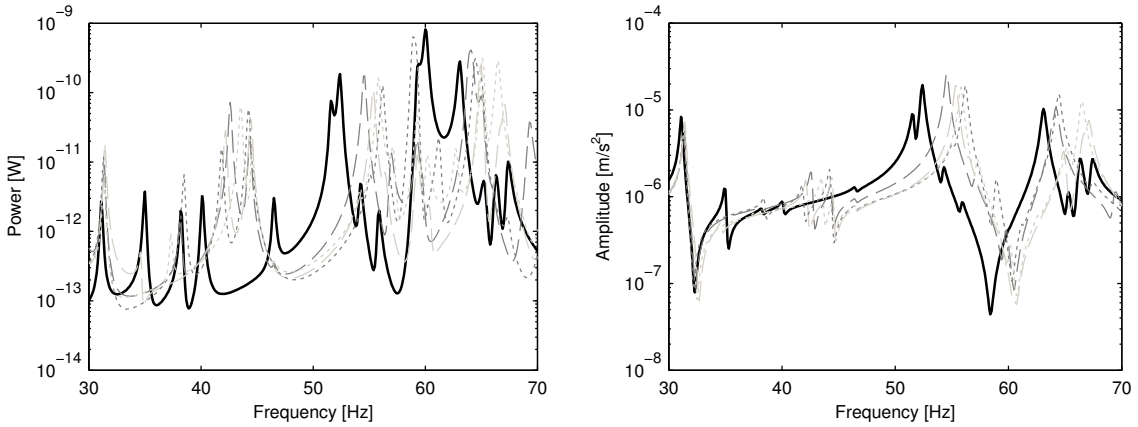

(a) Power flow transmitted at the interface

(b) Acceleration response level of the main core (vertical direction)

Figure 7: Results of the robust multi-objective optimization procedure : — initial ; optima —— 1, —— 2, ··· 3, ··· 4

Acknowledgments

This work has been funded by the Future Preparation - Research and Technology Sub-Directorate of the *Centre National d'Études Spatiales* (*CNES*) - Launchers Directorate (Paris, France).

REFERENCES

[1] B. Ait-Brik Une mthodologie de conception robuste en dynamique des structures. *European Journal of Computational Mechanics*, **15**, 15–27, 2006.

[2] L.-O. Gonidou, Dynamic characterization of structural interfaces. *Proceedings of the Spacecraft and Launch Vehicle Dynamic Environments Workshop*, 2007.

[3] Y.I. Bobrovnitskii, Some energy relations for mechanical systems. *IUTAM Symposium on Statistical Energy Analysis*, Southampton, United-Kingdom, 1997.

[4] H.G.D. Goyder and R.G. White, Vibrational power flow from machines into built-up structures, Part III: Power flow through isolation systems. *Journal of Sound and Vibration*, **68**, 97–117, 1980.

[5] MathWorks, *Optimization Toolbox - User's guide, R2012a*, 2012

[6] G. Masson, B. Ait Brik, S. Cogan and N. Bouhaddi, Component mode synthesis (CMS) based on an enriched Ritz approach for efficient structural optimization. *Journal of Sound and Vibration*, **296**, 845–860, 2006.

[7] D.W. Miller, S.R. Hall, A.H. von Flotow, Optimal control of power flow at structural junctions. *Journal of Sound and Vibration*, **140**, 475–497, 1990.

[8] R.J. Pinnington and D.C.R. Pearce, Multipole expansion of the vibration transmission between a source and a receiver. *Journal of Sound and Vibration*, **142**, 461–479, 1990.

[9] N. Srinivas and K. Deb, Multiobjective optimization using nondominated sorting in genetic algorithms. *Evolutionary Computation*, **2**, 221–248, 1994.

[10] J. Su, A.T. Moorhouse and B.M. Gibbs, Towards a practical characterization for structure-borne sound sources based on mobility techniques. *Journal of Sound and Vibration*, **185**, 737–741, 1995.

[11] P. Vinot and S. Cogan, Procedure for initializing interface stiffness based on sensitizing inputs. *AIAA Journal*, **42**, 1246–1251, 2004.

[12] T. Weisser, E. Foltête, N. Bouhaddi and L.-O. Gonidou A power flow mode approach dedicated to structural interface dynamic characterization. *Jounral of Sound and Vibration*, **334**, 202–218, 2015.